

STUDIES OF THERMOMETRIC MATERIAL $\text{Lu}_{1-x}\text{Zr}_x\text{NiSb}$

Volodymyr Pashkevych, Ph. Dr., *Volodymyr Krayovskyy*, Dr. Sc., Prof., As.-Prof.,

Mariya Rokomanyuk, PhD-student, *Petro Haranuk*, Ph. Dr., As.-Prof.,

Volodymyr Romaka, Dr. Sc., Prof.,

Lviv Polytechnic National University, Ukraine

Yuriy Stadnyk, Ph. Dr., Senior Scientist, *Lyubov Romaka*, Ph. Dr., Senior Scientist,

Andriy Horyn, Ph. Dr., Senior Research,

Ivan Franko National University of Lviv, Ukraine

Daniel Fruchart, Dr. Sc., Prof.

Research Director Neel Institute CNRS Grenoble France;

e-mail: vkrayovskyy@ukr.net

Abstract. The results of experimental research of perspective thermometric material $\text{Lu}_{1-x}\text{Zr}_x\text{NiSb}$ which can be used for the production of sensitive elements of thermoelectric and electroresistive thermometers are presented.

Thermometric materials $\text{Lu}_{1-x}\text{Zr}_x\text{NiSb}$, $x=0.01-0.10$, were made by fusing a charge of components in an electric arc furnace with a tungsten electrode (cathode) in an atmosphere of purified argon under a pressure of 0.1 kPa on a copper water-cooled hearth (anode). Heat treatment of alloys consisted of homogenizing annealing at a temperature of 1073 K. Annealing of samples was carried out for 720 h in vacuumed up to 1.0 Pa ampoules of quartz glass in muffle electric furnaces with temperature control with an accuracy of ± 10 K. Diffraction arrays were obtained on a diffractometer DRON-4.0 (FeK α radiation), and the structural characteristics of $\text{Lu}_{1-x}\text{Zr}_x\text{NiSb}$ were calculated using the Fullprof program. The chemical and phase compositions of the samples were monitored using a scanning electron microscope (Tescan Vega 3 LMU).

The study of the temperature dependences of the resistivity $\rho(T,x)$ and the thermopower coefficient $\alpha(T,x)$ of $\text{Lu}_{1-x}\text{Zr}_x\text{NiSb}$ was performed in the temperature range of 80–400 K on samples in the form of rectangular parallelepipeds measuring $\sim 1.0 \times 1.0 \times 5.0$ mm³. Measurements of the values of the specific magnetic susceptibility $\chi(x)$ of $\text{Lu}_{1-x}\text{Zr}_x\text{NiSb}$ samples were performed by the relative Faraday method at a temperature of 273 K using a thermogravimetric installation with an electronic microbalance EM-5-ZMP in magnetic fields up to 10 kGs.

Microprobe analysis of the concentration of atoms on the surface of $\text{Lu}_{1-x}\text{Zr}_x\text{NiSb}$ samples, $x=0.01-0.10$, established their correspondence to the initial compositions of the charge, and X-ray phase analysis showed no traces of extraneous phases on the sample diffractograms, except for the main phase.

The nonmonotonic nature of the change in the values of the unit cell period of the thermometric material $a(x)$ of $\text{Lu}_{1-x}\text{Zr}_x\text{NiSb}$, $x=0.01-0.10$, which differs from the results of modeling structural characteristics using software packages AkaiKKR and Elk. The nonmonotonic change in the values of the period of the unit cell $a(x)$ of $\text{Lu}_{1-x}\text{Zr}_x\text{NiSb}$ and the presence of the extremum dependence suggests that the impurity Zr atoms introduced into the matrix of the LuNiSb basic semiconductor can simultaneously occupy partially different crystallographic positions in different ratios.

The temperature resistivities ρ and the thermopower coefficient α of the LuNiSb base semiconductor contain high- and low-temperature activation regions, which is characteristic of doped and compensated semiconductors. The introduction into the LuNiSb structure of the lowest concentration of impurity Zr atoms in the experiment ($x=0.01$) radically changes both the behavior of the temperature dependences of the resistivity ρ and the thermopower coefficient α and the type of the main electric current carriers. The values of the resistivity $\rho(T,x)$ of $\text{Lu}_{1-x}\text{Zr}_x\text{NiSb}$ only increase with increasing temperature, which is characteristic of the metallic type of electrical conductivity and is due to the mechanisms of scattering of current carriers. This nature of the change in electrical resistance $\rho(T,x)$ is evidence that the Fermi level ε_F has left the bandgap ε_g and is in the conduction band ε_c . This is indicated by the negative values of thermopower coefficient $\alpha(T,x)$ at all concentrations and temperatures.

Studies of the magnetic susceptibility $\chi(x)$ showed that the samples as a basic semiconductor LuNiSb , as well as the thermometric material $\text{Lu}_{1-x}\text{Zr}_x\text{NiSb}$, at all concentrations of impurities Zr, are Pauli paramagnetic. There is a synchronicity of the behavior of $\chi(x)$ with the dependences of the resistivity $\rho(x, T)$ and the thermopower coefficient $\alpha(x, T)$, which is due to the change in the density of states at the Fermi level $g(\varepsilon_F)$.

The results of experimental studies of the $\text{Lu}_{1-x}\text{Zr}_x\text{NiSb}$ thermometric material completely coincide with the results of modeling its kinetic characteristics under the presence of vacancies in the crystallographic positions 4a and 4c of the Lu and Ni atoms, respectively. Such studies allow making adjustments in the structural studies of thermometric material with an accuracy that significantly exceeds the accuracy of X-ray research methods. The obtained results will allow us to clarify the spatial arrangement of atoms in the nodes of the unit cell, as well as to identify the mechanisms of electrical conductivity to determine the conditions for the synthesis of thermosensitive materials with maximum efficiency of thermal energy conversion into electricity.

Keywords: Electric conductivity, Thermopower coefficient, Fermi level.

1. Introduction

The presented work is a continuation of the study of a new semiconductor thermometric material $\text{Lu}_{1-x}\text{Zr}_x\text{NiSb}$, started in [1] by modeling its structural,

thermodynamic, kinetic, and energy characteristics. Modeling of the electronic structure of $\text{Lu}_{1-x}\text{Zr}_x\text{NiSb}$ was performed by two methods: Koring-Kon-Rostocker (KKR) method, AkaiKKR software package [2] in the

coherent potential approximation and full-potential linearized plane wave method (FLAPW), Elk software package [3].

The study of the methods of entry of Zr atoms into the matrix of the basic LuNiSb semiconductor and their occupation of different positions, as well as the presence of vacancies in them, showed that the most acceptable results of experimental studies [4–7] are a model of electronic structure that assumes vacancies in crystallographic positions $4a$ of Lu atoms (0.005) and $4c$ of Ni atoms (~ 0.04).

Modeling on this basis of the kinetic characteristics of the semiconductor thermometric material $\text{Lu}_{1-x}\text{Zr}_x\text{NiSb}$, in particular, the temperature dependences of the resistivity $\rho(T,x)$ and the thermopower coefficient $\alpha(T,x)$ showed that at the lowest concentrations of Zr atoms the Fermi level in ε_F is located conductivity ε_C . This is indicated by the negative values of the thermopower coefficient $\alpha(T,x)$ and the metallic type of electrical conductivity of the thermometric material $\text{Lu}_{1-x}\text{Zr}_x\text{NiSb}$. This changes the type of the main current carriers from the holes to the electrons.

The paper presents the results of experimental studies of the thermometric material $\text{Lu}_{1-x}\text{Zr}_x\text{NiSb}$, which will establish the correctness of the methods used to model its structural, thermodynamic, energy, and kinetic characteristics obtained by doping the basic semiconductor LuNiSb with Zr atoms by replacing Lu atoms ($4a$). The obtained results will allow us to clarify the spatial arrangement of atoms in the nodes of the unit cell, as well as to identify the mechanisms of electrical conductivity to determine the conditions for the synthesis of thermosensitive materials with maximum efficiency of thermal energy conversion into electricity.

2. Disadvantages

Studies of thermometric materials based on the basic semiconductor RNiSb [4–7] have established their high sensitivity to heat treatment (temperature and duration of annealing).

3. Aim of the Study

To establish the mechanism of formation of structural defects in the thermometric material $\text{Lu}_{1-x}\text{Zr}_x\text{NiSb}$, which will allow to identify the mechanisms of electrical conductivity and to determine the conditions of their synthesis.

4. Research methods

Thermometric materials $\text{Lu}_{1-x}\text{Zr}_x\text{NiSb}$, $x=0.01\text{--}0.10$, were made by fusing a charge of components weighed with an accuracy of ± 0.001 g in an electric arc furnace with a tungsten electrode (cathode) in an atmosphere of purified argon at a pressure of 0.1 kPa on a copper water-cooled pod. Pre-alloyed spongy titanium was used

as the hetero. To achieve homogeneity, the alloys were remelted twice. Control of charge losses during melting was performed by repeated weighing. Heat treatment of alloys consisted of homogenizing annealing at a temperature of 1073 K. Annealing of samples was carried out for 720 h in vacuum-packed up to 1.0 Pa ampoules of quartz glass in muffle electric furnaces with temperature control with an accuracy of ± 10 K. Diffraction data arrays were obtained on powder diffractometer DRON-4.0 (FeK α radiation), and with the help of Fullprof [8], the structural characteristics of $\text{Lu}_{1-x}\text{Zr}_x\text{NiSb}$ were calculated. The chemical and phase compositions of the samples were monitored by metallographic analysis (scanning electron microscope Tescan Vega 3 LMU).

The study of the temperature dependences of the resistivity $\rho(T,x)$ and the thermopower coefficient $\alpha(T,x)$ $\text{Lu}_{1-x}\text{Zr}_x\text{NiSb}$ was performed in the temperature range of 80–400 K on samples in the form of rectangular parallelepipeds measuring $\sim 1.0 \times 1.0 \times 5$ mm³. The values of the electrical resistance were measured using the four-contact method, and the values of the thermopower coefficient by the potentiometric method concerning copper. To reduce the "parasitic" effects caused by the influence of thermo-emf at the points of contact, as well as the effects caused by the possible influence of the p - n junction, the voltage drop on the sample was measured at different directions of electric current [9]. Measurements of the values of the specific magnetic susceptibility $\chi(T,x)$ of $\text{Lu}_{1-x}\text{Zr}_x\text{NiSb}$ samples were performed by the relative Faraday method at a temperature of 273 K using a thermogravimetric installation with an electronic microbalance EM-5-ZMP in magnetic fields up to 10 kGs.

5. Investigation of structural characteristics of thermometric material $\text{Lu}_{1-x}\text{Zr}_x\text{NiSb}$

Microprobe analysis of the concentration of atoms on the surface of $\text{Lu}_{1-x}\text{Zr}_x\text{NiSb}$, $x=0.01\text{--}0.10$, established their correspondence to the initial compositions of the charge, and X-ray phase analysis showed no traces of extraneous phases on the sample diffractograms, except for the main phase. It should be noted that the manufactured thermometric materials $\text{Lu}_{1-x}\text{Zr}_x\text{NiSb}$, $x=0.01\text{--}0.10$, are within the concentrations of solid substitution solution and coincide with the results of modeling thermodynamic characteristics [1].

Since the atomic radius Lu ($r_{\text{Lu}}=0.173$ nm) predominates in Zr ($r_{\text{Zr}}=0.160$ nm), the values of the period of the unit cell $a(x)$ of the thermometric material $\text{Lu}_{1-x}\text{Zr}_x\text{NiSb}$ were expected to decrease if the Lu atoms were replaced by Zr atoms. By the way, such a result was shown by modeling the structural characteristics of $\text{Lu}_{1-x}\text{Zr}_x\text{NiSb}$ using the software packages AkaiKKR and Elk [2, 3] (fig. 1, insert). However, the results of X-ray structural studies of the thermometric material $\text{Lu}_{1-x}\text{Zr}_x\text{NiSb}$ differ significantly from the simulation

results [1]. As we can see from Fig. 1, in the area of concentrations $x=0-0.02$, the values of the period of the cell $a(x)$ $\text{Lu}_{1-x}\text{Zr}_x\text{NiSb}$ increase rapidly, pass through the maximum, and decrease equally rapidly at $x>0.02$.

The fact that there is a nonmonotonic change in the values of the period of the unit cell $a(x)$ $\text{Lu}_{1-x}\text{Zr}_x\text{NiSb}$ (Fig. 1) and the presence of the extremum dependence suggests that the impurity Zr atoms introduced into the matrix of the basic semiconductor LuNiSb can simultaneously in different ratios occupy both different positions and generate the appearance of vacancies or atoms in the tetrahedral voids of the structure, which make up $\sim 24\%$ of the volume of the unit cell [4].

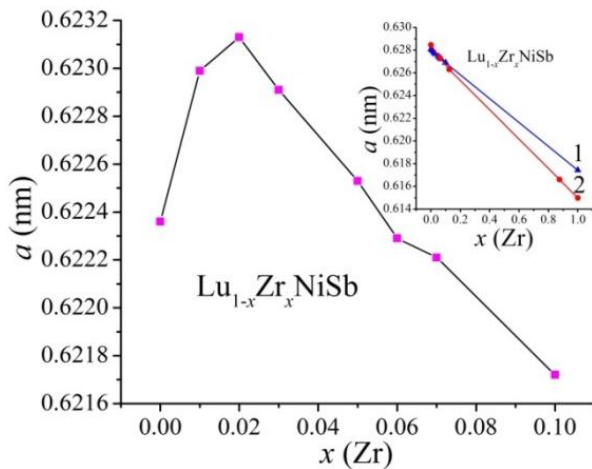


Fig. 1. Experimental measurements of the values of the period of the unit cell $a(x)$ of the thermometric material $\text{Lu}_{1-x}\text{Zr}_x\text{NiSb}$. Insert: simulation of $a(x)$ by AkaiKKR (1) and Elk (2) methods [1]

We can assume that the increase in the values of the period of the unit cell $a(x)$ $\text{Lu}_{1-x}\text{Zr}_x\text{NiSb}$ in the region of concentrations $x=0-0.02$ is caused by the return of Ni atoms to their crystallographic position and the occupation of available vacancies. After all, the results of modeling the energy characteristics of the basic LuNiSb semiconductor showed the existence of vacancies in the crystallographic position of $4c$ Ni atoms.

Alternatively, based on the fact that the atomic radius of the Ni atom ($r_{\text{Ni}}=0.124$ nm) is the smallest among the chemical elements of the thermometric material $\text{Lu}_{1-x}\text{Zr}_x\text{NiSb}$ ($r_{\text{Sb}}=0.159$ nm), increasing the values of $a(x)$ $\text{Lu}_{1-x}\text{Zr}_x\text{NiSb}$ may cause partial occupation of impurities Zr crystallographic position of $4c$ atoms of Ni. However, given the significant difference in the atomic radii of Ni and Zr, such a substitution seems unlikely.

Therefore, there are some variants of structural changes of the $\text{Lu}_{1-x}\text{Zr}_x\text{NiSb}$ thermometric material, which are accompanied by an increase in the values of the period of the cell $a(x)$ when Zr atoms are introduced into the LuNiSb semiconductor structure.

Thus, the introduction of Zr atoms ($4d^25s^2$) into the LuNiSb structure by substituting Lu ($5d^16s^2$) atoms at position $4a$ should generate structural defects of donor nature, since the Zr atom contains more d -electrons than the Lu atom. In this case, an impurity donor zone ε_D will appear in the bandgap of the semiconductor. In the case of substitution of Ni atoms ($3d^84s^2$) by Zr atoms, structural defects of acceptor nature must be formed in the crystal, because the Zr atom contains fewer d -electrons. At the same time, the ε_A acceptor zone should appear in the $\text{Lu}_{1-x}\text{Zr}_x\text{NiSb}$ band gap. In this case, the thermometric material $\text{Lu}_{1-x}\text{Zr}_x\text{NiSb}$, $x=0-0.02$, will simultaneously contain donors and acceptors, and their ratio will be determined by the sign of the thermopower coefficient $\alpha(T,x)$ and the type of main current carriers.

On the other hand, if we recall the results of modeling the energy characteristics of the basic semiconductor LuNiSb [1], which indicated the existence of vacancies in positions $4a$ and $4c$ of Lu and Ni atoms, respectively, the occupation of Zr atoms vacancies in position $4a$ or Ni or Zr atoms vacancies in position $4c$ will lead to the generation of structural defects of donor nature, and impurity donor zones ε_D will appear in the forbidden zone. At the same time, structural defects of acceptor nature disappear (vacancies disappear) and the corresponding ε_A acceptor zones.

The following results of the study of electrokinetic, energy, and magnetic characteristics of the thermometric material $\text{Lu}_{1-x}\text{Zr}_x\text{NiSb}$, $x=0-0.10$, and their comparison with the results of modeling such characteristics [1], will identify the mechanisms of electrical conductivity and conditions for obtaining effective thermometric materials.

6. Investigation of kinetic, energy, and magnetic characteristics of thermometric material $\text{Lu}_{1-x}\text{Zr}_x\text{NiSb}$

Temperature and concentration dependences of resistivity ρ and thermopower coefficient α of thermometric materials $\text{Lu}_{1-x}\text{Zr}_x\text{NiSb}$ are shown in Fig. 2-4. As can be seen from fig. 2, for the basic semiconductor LuNiSb the change in the values of the resistivity with temperature is characteristic of semiconductors [9] and is described by relation (1):

$$r^{-1}(T) = r_1^{-1} \exp\left\{-\frac{\varepsilon_1}{k_B T}\right\} + r_3^{-1} \exp\left\{-\frac{\varepsilon_3}{k_B T}\right\} \quad (1)$$

where the first high-temperature term describes the activation of current carriers e_1^r from the Fermi level ε_F to the level of continuous energy zones, and the second, low-temperature term, the hopping conductivity at impurity donor states e_2^r with energies close to the Fermi level ε_F . It was calculated that in the basic LuNiSb semiconductor the Fermi level ε_F is located at a distance $\varepsilon_1^r = 10.2$ meV from the ceiling of the

valence band ε_V . Temperature dependences of the thermopower coefficient $\alpha(1/T)$ LuNiSb (fig. 2) can be described using expression (2):

$$a = \frac{k_B}{e} \frac{\alpha \varepsilon_i^a}{\varepsilon k_B T} - g + 1 + \frac{\gamma}{\gamma} \quad (2)$$

where γ is a parameter that depends on the nature of the scattering mechanism [9]. From high- and low-temperature activation regions of the $\alpha(1/T)$ LuNiSb dependence, the values of activation energies $\varepsilon_1^a = 35.3$ meV and $\varepsilon_2^a = 1.9$ meV were calculated, respectively, which

are proportional to the amplitude of large-scale fluctuations of zones of continuous energies and small-scale flux.

The existence of a high-temperature activation region on the temperature dependence of the resistivity $\ln(\rho(1/T))$ of LuNiSb (fig. 2a) indicates the location of the Fermi level ε_F in the bandgap ε_g near the valence band ε_V . (fig. 2b) We can say that in the basic semiconductor LuNiSb holes are the main current carriers, which is consistent with the results of modeling the energy characteristics [1] and the results of previous studies [[4–7].

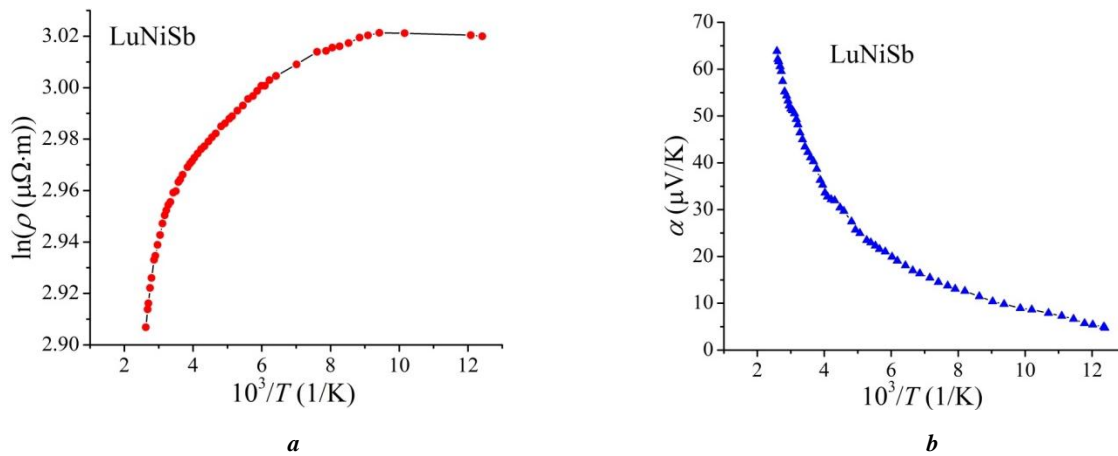


Fig. 2. Temperature dependences of the resistivity $\ln(\rho(1/T))$ (a) and the thermopower coefficient $\alpha(1/T)$ (b) of the basic semiconductor LuNiSb

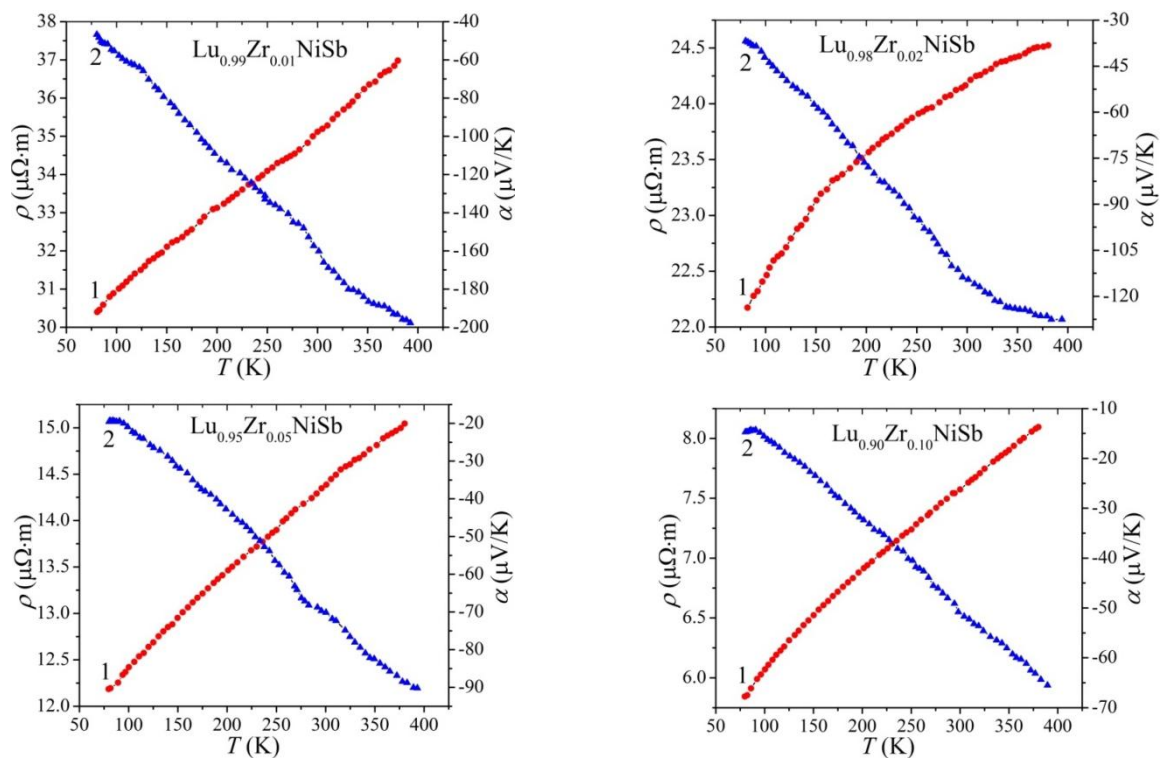


Fig. 3. Temperature dependences of specific electrical resistance $\rho(T,x)$ and thermopower coefficient $\alpha(T,x)$ $\text{Lu}_{1-x}\text{Zr}_x\text{NiSb}$

The metallic nature of the electrical conductivity of the thermometric material $\text{Lu}_{1-x}\text{Zr}_x\text{NiSb}$ was predicted even at the lowest concentration of Zr impurity in the simulation of kinetic characteristics, provided that there are vacancies in the crystallographic positions 4a and 4c of the Lu and Ni atoms.

In the absence of such vacancies, the calculations showed that if $\text{Lu}_{1-x}\text{Zr}_x\text{NiSb}$ is replaced by Lu atoms by Zr atoms, which generates structural defects of donor nature, then only at a concentration of $x \approx 0.02$ the Fermi level ε_F was near the middle of the bandgap ε_g . At the temperature dependences of the resistivity $\ln(\rho(1/T, x))$ of $\text{Lu}_{1-x}\text{Zr}_x\text{NiSb}$, we would observe high-temperature activation regions formed by the activation of current carriers from the Fermi level ε_F in the zones of continuous energies, and only at concentrations of $\text{Lu}_{1-x}\text{Zr}_x\text{NiSb}$, $x > 0.04$, the Fermi level ε_F crosses the bottom of the conduction band, and the activation regions disappear at the temperature dependences of the resistivity $\ln(\rho(1/T))$.

The behavior of the resistivity $\rho(x, T)$ of $\text{Lu}_{1-x}\text{Zr}_x\text{NiSb}$ at all temperatures (fig. 4) also corresponds to the results of modeling the kinetic characteristics under vacancies at the positions of Lu and Ni atoms. If the semiconductor simultaneously contains carriers of electric current of both types (electrons and holes), then the maximum on the dependence $\rho(x, T)$ of $\text{Lu}_{1-x}\text{Zr}_x\text{NiSb}$ shows that the concentrations of acceptors and donors are the same. In the absence of such vacancies, the maximum on the dependence $\rho(x, T)$ should be at a concentration of $x \approx 0.02$, when the Fermi level ε_F will be near the middle of the bandgap ε_g . The maximum $\rho(x, T)$ of $\text{Lu}_{1-x}\text{Zr}_x\text{NiSb}$ for $x \approx 0.01$ cannot be considered as the maximum of the dependence in the range $x = 0 - 0.10$. The values of electrical resistance for $x = 0$ and $x \geq 0.01$ do not belong to one dependence. After all, for $x = 0$ we have a semiconductor material of hole type conductivity when the Fermi level ε_F lies at a distance of 10.2 meV from the edge of the valence band ε_V , and at a concentration of $x = 0.01$ it is located deep in the conduction band ε_C and electrons are the main current carriers.

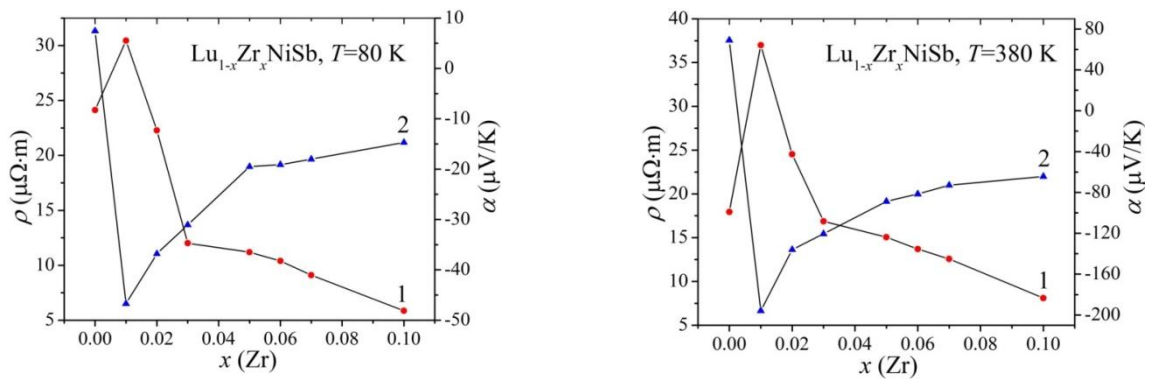


Fig. 4. Change in the values of resistivity $\rho(x, T)$ (1) and the thermopower coefficient $\alpha(x, T)$ (2) $\text{Lu}_{1-x}\text{Zr}_x\text{NiSb}$ at different temperatures

The same applies to the nature of the change in the values of the thermopower coefficient $\alpha(x, T)$ of $\text{Lu}_{1-x}\text{Zr}_x\text{NiSb}$, in particular, the available minimum at $x \approx 0.01$ (fig. 4). It is correct to talk only about the decrease in the values of $\rho(x, T)$ and the increase in the values of $\alpha(x, T)$ of $\text{Lu}_{1-x}\text{Zr}_x\text{NiSb}$ in the concentration range $0.01 \leq x \leq 0.10$ at all temperatures (fig. 4), which indicates an increase in electron concentration and density states at the Fermi level $g(\varepsilon_F)$. This is understandable, because Zr atoms, replacing Lu, generate defects of donor nature, which supply electrons to the semiconductor.

It is known that the values of the activation energy $\varepsilon_1^a(x)$, calculated from the low-temperature activation regions of the thermopower coefficient $\alpha(1/T)$ of $\text{Lu}_{1-x}\text{Zr}_x\text{NiSb}$, allow us to establish the degree of compensation of the semiconductor material. After all, the values of $\varepsilon_1^a(x)$ are proportional to the amplitude of

large-scale fluctuations of zones of continuous energies caused by the fluctuational nature of the location in the crystal space of charged centers, in particular, ionized acceptors and donors [9]. The higher the degree of semiconductor compensation (ratio of ionized acceptors and donors), the greater the distortion of the zones of continuous energies and the value of the amplitude of modulation of the zones of continuous energies $\varepsilon_1^a(x)$. Note that it is correct to analyze the behavior of the activation energy $\varepsilon_1^a(x)$ of $\text{Lu}_{1-x}\text{Zr}_x\text{NiSb}$ only at concentrations of $0.01 \leq x \leq 0.10$, when the conductivity of the material determines one type of carrier. After all, for $x = 0$ we have a semiconductor of hole type, and for $0.01 \leq x$ – electronic.

From fig. 5 shows that at concentrations of $0.01 \leq x \leq 0.10$ the values of the activation energy $\varepsilon_1^a(x)$ of $\text{Lu}_{1-x}\text{Zr}_x\text{NiSb}$ rapidly decrease, indicating the

predominance of the concentration of one type of electric current carriers over another. Since the main carriers of $\text{Lu}_{1-x}\text{Zr}_x\text{NiSb}$ current at $0.01 \leq x$ are electrons and their concentration is much higher than that of holes, the degree of compensation decreases with increasing impurity concentration.

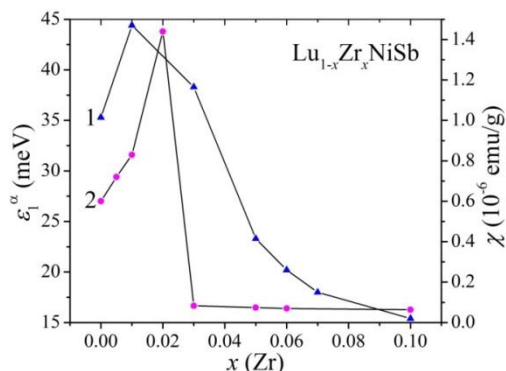


Fig. 5. Change in the values of activation energy $\epsilon_1^a(x)$ (1) and specific magnetic susceptibility $\chi(x, 273 \text{ K})$ (2) thermometric material $\text{Lu}_{1-x}\text{Zr}_x\text{NiSb}$

Typically, when doping a hole-type semiconductor with donors, electrons are first captured by acceptors to concentrations when the number of acceptors corresponds to the number of ionized donors. When all acceptors are ionized, the electrons supplied by the donors become free and participate in the electrical conductivity. That is, first the electrons are captured by the acceptors present in the semiconductor [9].

Studies of the magnetic susceptibility $\chi(x)$ showed that the samples as the basic semiconductor LuNiSb , as well as the thermometric material $\text{Lu}_{1-x}\text{Zr}_x\text{NiSb}$, at all concentrations of the impurity Zr, are Pauli paramagnetic (fig. 5, dependence 2). Therefore, the synchrony of the behavior of $\chi(x)$ with the dependences of the resistivity $\rho(x, T)$ and the thermopower coefficient $\alpha(x, T)$ (fig. 4), associated with the change in the density of states at the Fermi level $g(\epsilon_F)$.

Therefore, the results of experimental studies of the $\text{Lu}_{1-x}\text{Zr}_x\text{NiSb}$ thermometric material completely coincide with the results of modeling its kinetic characteristics under the presence of vacancies in the crystallographic positions 4a and 4c of the Lu and Ni atoms, respectively. Such studies allow making adjustments in the structural studies of thermometric material with an accuracy that significantly exceeds the accuracy of X-ray research methods. The obtained results will allow us to clarify the spatial arrangement of atoms in the nodes of the unit cell, as well as to identify the mechanisms of electrical conductivity to determine the conditions for the synthesis of thermosensitive materials

with maximum efficiency of thermal energy conversion into electricity.

7. Conclusions

Based on the results of the study of structural, kinetic, energy, and magnetic characteristics of samples of thermometric material $\text{Lu}_{1-x}\text{Zr}_x\text{NiSb}$, $x=0-0.10$, it is established that the obtained results completely coincide with the results of modeling kinetic characteristics provided vacancies in crystallographic positions 4a and 4c of Lu atoms and Ni, accordingly. These results give an adequate picture of the spatial arrangement of atoms in the units of the unit cell of the material $\text{Lu}_{1-x}\text{Zr}_x\text{NiSb}$, $x=0-0.10$, and also allow to identify the mechanisms of electrical conductivity to determine the conditions of synthesis of thermometric materials with maximum efficiency of thermal energy conversion.

8. Gratitude

The authors express their gratitude to the members of the scientific seminar of the Department of Information and Measurement Technologies of Lviv Polytechnic National University for an interesting and meaningful discussion on the results of these studies.

9. Conflict of interest

The authors declare that there is no financial or other possible conflict related to this work.

References

- [1] V. Krayovskyy, V. Pashkevych, A. Horpenuk, V. A. Romaka, Yu. Stadnyk, L. Romaka, A. Horyn, V. V. Romaka, *Measuring Equipment and Metrology*, vol.82, no.4, p.12–17, 2021.
- [2] M. Schruter, H. Ebert, H. Akai, P. Entel, E. Hoffmann, G.G. Reddy, *Phys. Rev. B*, vol. 52, p. 188–209, 1995.
- [3] All-electron full-potential linearised augmented-plane wave (FP-LAPW). [Online]. Available: <http://elk.sourceforge.net>.
- [4] V. A. Romaka, Yu. Stadnyk, V. Krayovskyy, L. Romaka, O. Guk, V. V. Romaka, M. Mykyuchuk, A. Horyn, *The latest heat-sensitive materials and temperature transducers*. Lviv Polytechnic Publishing House, Lviv, 2020. [in Ukrainian].
- [5] Wolanska, K. Synoradzki, K. Ciesielski, K. Zaleski, P. Skokowski, D. Kaczorowski, *Mater. Chem. Phys.*, Vol.227, pp.29–36, 2019. [Online]. Available: <https://doi.org/10.1016/j.matchemphys.2019.01.056>
- [6] K. Synoradzki, K. Ciesielski, I. Veremchuk, H. Borrmann, P. Skokowski, D. Szymanski, Y. Grin, D. Kaczorowski, *Materials*. vol. 12, P. 1723–1730, 2019. [Online]. Available: <https://doi.org/10.3390/ma12101723>
- [7] K. J. Pierre, R. V. Skolozdra, *J. Alloys Compounds*, Vol. 265, pp. 42–50, 1998. ([https://doi.org/10.1016/S0925-8388\(97\)00419-2](https://doi.org/10.1016/S0925-8388(97)00419-2)).
- [8] T. Roisnel, J. Rodriguez-Carvajal. WinPLOTR: a Windows Tool for Powder Diffraction Patterns analysis, *Mater. Sci. Forum*, Proc. EPDIC7, vol. 378–381, p. 118–123, 2001. (<https://doi.org/10.4028/www.scientific.net/MSF.378-381.118>).

[9] B. I. Shklovskii, A. L. Efros. *Electronic Properties of Doped Semiconductors*. NY, Springer-Verlag, 1984. (<http://doi10.1007/978-3-662-02403-4>).